

## GRAVITATIONAL SEDIMENTATION DISTORTIONS OF THE PARTICLE SIZE SPECTRUM AND PROFILES OF LIGHT SCATTER- ING PARAMETERS IN THE ATMOSPHERIC MIXING LAYER

R.F. Rakhimov

*Institute of Atmospheric Optics,  
Siberian Branch of the Academy of Sciences of the USSR, Tomsk  
Received November 29, 1989*

*A technique is described to simulate numerically the variability of the aerosol light scattering parameters in the daytime atmospheric mixing layer. Some results of model estimations of the effect of gravitational sedimentation upon the optical properties of surface atmospheric hazes are presented.*

Diurnal variations of the atmospheric temperature field induced by changes in the radiative heat flux divergence not only alter the local state of the aerosol phase by changing the ambient relative humidity, but produce a noticeable spatial redistribution of the concentration of dispersed particles.

The removal efficiency of aerosols and aerosol generating substances from the underlying surface, like that of other optically active components, and their transport into the free atmosphere are governed by the intensity of eddy mixing in the lower atmospheric layers.

### THE MIXING LAYER MODEL

Nighttime cooling of the surface atmospheric layer contributes to the formation of a temperature inversion, reaching 70–150 m by the morning hours (this layer is shown schematically by a dashed line in Fig. 1); this inversion suppresses diffusion in the surface layer. The stronger daytime thermal component of eddy diffusion stimulates exchange processes and leads to the formation of an unstable mixing layer (ML), topped by a temperature inversion; the thickness of this layer gradually increases during the day (see Fig. 1b).

A theoretical model of ML, first suggested by Boll<sup>2</sup> and refined in further studies by Lilly and Tennekes,<sup>1,3</sup> describes the state of the layer elements by the following system of equations:

$$h \frac{d\Theta}{dt} = \langle w'\Theta' \rangle_0 - \langle w'\Theta' \rangle_h; \quad (1)$$

$$\Delta \frac{d\Theta}{dt} = - \langle w'\Theta' \rangle_h; \quad (2)$$

$$\frac{d\Theta}{dt} = - \frac{d\Theta}{dz} + \gamma \frac{d\Theta}{dz}; \quad (3)$$

$$\langle w'\Theta' \rangle_h = - c \langle w'\Theta' \rangle_0 \quad (4)$$

where  $h$  is the mixing layer thickness;  $\Delta$  is the temperature drop at the inversion base;  $\gamma$  is the lapse rate of the potential temperature  $\Theta$  above the layer;  $\langle w'\Theta' \rangle_0$  and  $\langle w'\Theta' \rangle_h$  are the average eddy heat fluxes at the surface and at the inversion base, respectively;  $c$  is the entrainment constant.

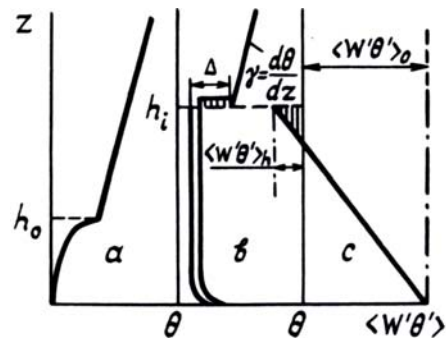


FIG. 1. Schematic presentation of model vertical profiles of potential temperature and eddy heat flux within and without the convective mixing layer.

The high rate of eddy mixing of the enthalpy, as the heat flows into the layer. Justifies the principal assumption of the model, namely, that the potential temperature profile suffers a parallel shift without any change in its shape during the day (see Fig. 1b).

To solve the system (1)–(4) diurnal variations in heat flux from the surface were approximated by a sine wave having its minimum at sunrise and its maximum at noon

$$\langle w'\Theta' \rangle_0 = B \sin[\omega (t - t_s)], \quad (5)$$

Here  $t_s$  is the moment of sunrise;  $B$  is the oscillation amplitude;  $\omega$  is the frequency of the diurnal cycle

$$\omega = \pi / (24 - 2t_s), \quad (6)$$

A significant element of this model is the so-called "entrainment problem", i.e., the question of the intensity of the entrainment of the warmer sub-inversion air masses into the structure of the mixing layer. Relationship (4), based on numerical empirical data, was used as the simplest hypothesis to close the system of equations (1)–(3). It postulates proportionality of eddy heat fluxes at both the base and top of the mixing layer. According to field observations the entrainment constant  $c$  in relationship (4) varies from 0 to 1, depending on the specific situation. The basic statistics of published observational data places  $c$  into the range 0.1–0.3. We assumed  $c = 0.2$  for our model calculations.

Thus, for specific boundary conditions, including the initial values of  $h_0$ ,  $\Theta_0$ ,  $\Delta_0$ , the model makes it possible to forecast diurnal variations of the layer elevation, the potential temperature distortion, and also the inversion depth  $\Delta(t)$ .

Figure 2 presents results from model estimates, illustrating the dynamics of the temporal variations for  $h(t)$ ,  $\Theta(t)$  for different  $B$  — the oscillation amplitude for  $\langle \omega' \Theta' \rangle_0$ . Note the nonlinear character of both dependences, which is especially pronounced for stronger eddy heat fluxes.

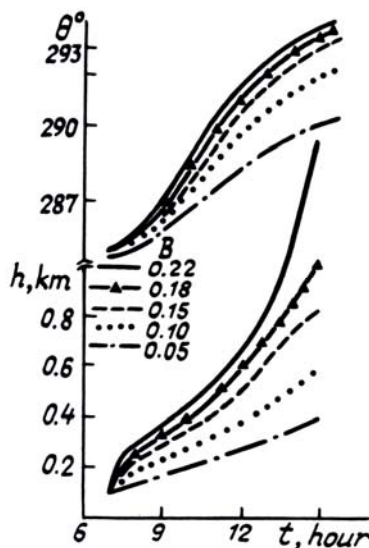


FIG. 2. Temporal dynamics of variations in height and potential temperature of the mixing layer for various amplitudes of the eddy heat flux variations.

Computations using the model (1)–(4) also demonstrate that in its upward movement the temperature inversion can reach a height of 2.5–3.0 km, provided the heat flux  $B$  is strong enough (in the range of 0.25–0.35 deg · m/s), and the conditions outside the layer are appropriate. This conclusion is supported by observations in arid climatic zones.<sup>7</sup> Consequently, the necessity for taking the interaction between the ML and the outer tropospheric layers into consideration becomes obvious.

As a first approximation to actual atmospheric situations we have considered the model of the process when the ML, as a sublayer of increased aerosol turbidity, is developing against the background of an ordinary level of dispersed phase content. This background aerosol was described by exponential profiles of its particle size spectrum integral parameters. During such modeling we tested the data used previously in Ref. 4 (see Table 2.6a, p. 39) as the starting print for the background optical model.

### THE ATMOSPHERIC HAZE PARTICLE SIZE SPECTRUM MODEL

Both the vertical structure of eddy fluxes and redistribution processes of the dispersed phase within the stratification, including the degree of layer loading, are closely related to the height of the mixing layer. Meanwhile, changes in potential temperature produce local variations in relative humidity.

In both cases the atmospheric haze particle size spectrum is modified. In the first case such modification results from processes taking place within the dispersed phase itself, while in the second case it results from local exchange processes between the aerosol particles and their environment.

To model both effects jointly we employed a technique of reductional description of the aerosol particle size spectrum.

The fractional method of determining the dispersed composition of atmospheric haze<sup>4</sup> makes it possible to employ integral parameters of its size spectrum, including  $V_1$ ,  $S_1$ ,  $N_1$  (the cumulative volumes, cross sections, and counted densities of separate size fractions), as predictors of the local optico-microphysical state of the aerosol phase. This noticeably simplifies modeling the dynamic transformation of the dispersed structure  $f(R, z, t)$  of the haze as affected by the considered processes. Here  $R$  is the radius of the aerosol particles;  $z$  is the running elevation above ground;  $t$  is the time.

The parameters  $R_1$ ,  $b_1$ , and  $A \cdot M_1$  of the function model of the size distribution of aerosol particles

$$f(R) = AR^{-3} \sum_{i=1}^3 M_i \exp\{-b_i [\ln(R/R_i)]^2\}, \quad (7)$$

needed to forecast the atmospheric optical characteristics, can be evaluated from the profiles of  $N_1(z, t)$ ,  $S_1(z, t)$ , and  $V_1(z, t)$ , employing in succession the relations<sup>4</sup>

$$R_1 = (3V_1)^{2/3} / [(4\pi N_1)^{1/6} \cdot S_1^{1/2}], \quad (8)$$

$$1/b_1 = \ln[(4\pi N_1)^{2/3} \cdot (3V_1)^{4/3} / S_1^2], \quad (9)$$

$$F_1 = A \cdot M_1 = S_1 / \sqrt{16\pi^3 / b_1}. \quad (10)$$

When modeling the spatial redistribution of the aerosol component, it was envisaged as a conserva-

tive component, i.e., the processes of internal transformation (mutual coagulation growth) were assumed to be incapable of significantly altering the size spectrum at an ordinary level of particle concentration over a period to 7–10 hours.<sup>5</sup> The increase of aerosol mass due to input from the environment (first of all due to atmospheric moisture) was accounted for at the second modeling stage, when light scattering properties of the aerosol were forecasted. An adjustment factor was then introduced to prescribe changes in the integral characteristics  $V_1$  and  $S_1$  with changing relative humidity. The semi-empirical Kasten and Hanel<sup>6</sup> dependence of the equilibrium particle size on relative humidity:

$$R = R_0 (1 - Q)^{\varepsilon_1} \quad (11)$$

was used here. Here  $Q$  is the relative humidity;  $\varepsilon_1$  is the of condensation activity parameter of a given aerosol fraction.

#### THE VERTICAL STRUCTURE OF HAZE: A FORECAST TECHNIQUE

To model structural dynamics of the atmospheric haze within an unstable ML, joint variations of the integral parameters of the particle size spectrum were forecasted. A dynamic equilibrium between the up- and downward fluxes of aerosol matter was assumed to be reached quickly enough during daytime development of ML at every level (of its eddy mixing regime), at least for the average values of the microphysical parameters.

Both the quasiequilibrium vertical aerosol profile within the layer and the respective vertical gradients of average integral characteristics of the overall dispersed structure must satisfy the condition of dynamic equilibrium between the particle number density, volume, and surface particle concentration fluxes. Note that these parameters are estimated for each separately taken fraction. In other words the balance between the fluxes of aerosol matter

$$D(z) \frac{d\chi}{dz} + \omega_1(z, R_1) \chi = 0 \quad (12)$$

is simultaneously satisfied for  $N_1$ ,  $S_1$ , and  $V_1$ . Here  $\chi(z)$  is understood as the average value of the given integral characteristic of the dispersed structure  $f(R, z)$ ;  $D(z)$  is the vertical profile of the eddy diffusion coefficient ( $\text{m}^2/\text{s}$ );  $\omega_1(z)$  is the average vertical velocity ( $\text{m}/\text{s}$ ) component of the ordered motion of the particles, related to the characteristic particle size in the given fraction.

In addition, during the first stage of numerical modeling of  $f(R, z, t)$  only spatial redistribution of aerosols is accounted for (while the layer integral loading is considered to remain at a quasiequilibrium level).

Thus, we assumed for the boundary conditions in Eq. (12)

$$\int_0^{h_1} \chi(z, t) dz = J_\chi = \text{const.} \quad (13)$$

where  $h_1$  was the running height of the mixing layer, and  $J_\chi$  was the integral content of aerosol particles in a unit atmospheric column within the layer, estimated for a specifically chosen characteristic.

In particular, this approach resulted in a noticeable drop in the surface optical density of the dispersed phase, not only because the layer was heated and the ambient relative humidity decreased, but also because the aerosol concentration itself was lowered. This was preceded by "dilution" of the aerosol turbidity due to the increasing height of the ML. Adjusting for stability of the layer, the vertical profile of the eddy diffusion coefficient was prescribed by the well known relationship<sup>8</sup>

$$D(z) = k u_* (1 - z/h_1)^2 / \Phi(z/L), \quad (14)$$

Here  $k$  is the Karman constant;  $u_*$  is the frictional velocity scale in the eddy flow;  $\Phi(z/L)$  is a semi-empirical function of the dimensionless stability parameter

$$\xi = z/L = -k \langle w'\theta' \rangle g(z + z_0) / \Theta u_*^3 \quad (15)$$

Here

$$L = \Theta u_*^3 / k \langle w'\theta' \rangle g \quad (16)$$

is the specific Monin–Obukhov length scale;  $g$  is the gravity acceleration;  $z_0$  is the roughness parameter for the underlying surface.

The estimates of  $u_*$ s to follow were obtained employing the logarithmic variation of the average wind speed  $\bar{u}(z)$  in the surface atmospheric layer<sup>9</sup>

$$\bar{u}(z) = \frac{u_*}{k} \ln \frac{z + z_0}{z_0} \quad (17)$$

The surface was assumed to be grass covered with  $z = 0.8$  cm. The average wind velocity measured at  $z = 3.0$  m was taken as the baseline  $\bar{u}$ .

According to Ref. 8, the form of the stability function  $A(\xi)$  depends on the argument range

$$A\Phi(\xi) = \begin{cases} 0.74 (1 - 9\xi)^{1/2}, & \xi \leq 0, \\ 0.74 (1 - 6.4\xi), & \xi > 0. \end{cases} \quad (18)$$

The Stokes gravitational sedimentation rate for aerosols is proportional to the squared radius of a particle<sup>9</sup> and is equal to

$$\omega_s(R) = 2\rho g R^2 C / 9\eta, \quad (19)$$

Here  $\eta$  is the viscosity coefficient of the medium,  $\rho$  is the density of the aerosol substance.

Prior to discussing other components  $\omega_1(z)$  we stress that such a dependence of the Stokes sedimentation rate on particle radius in the Earth's gravitational field is considered to be the principal cause of the aerosol size spectrum deformations: they are produced by spatial redistribution of haze particles within the ML.

The size range for particles forming the atmospheric haze extends from hundredths of a micron to several tens of microns, and the mean free path for molecules of gas at the surface is  $l \sim 0.07 \mu\text{m}$ . Therefore we have to account for the Cunningham adjustment factor  $C_C$  when computing the value of  $\omega_s$  from the relationship (18)

$$C_C = 1 + \frac{l}{R} \left[ 1.257 + 0.4 \exp \left[ -1.10 \frac{R}{l} \right] \right] \quad (20)$$

In addition, within the framework of the approach discussed, we operate with the so-called effective dry deposition rate, when considering scavenging out of particles from the eddy flux by various obstacles in the surface layer (i.e., elements of the surface roughness). This is an important sink mechanism for the dispersed phase in the ML.

In our computations we tested a linear dependence of the dry deposition rate on height

$$\omega_d(z) = \begin{cases} \alpha_d (L - z), & z < L, \\ 0, & z \geq L. \end{cases} \quad (21)$$

This linear dependence was also used to approximate the vertical velocity profile of the organized convective movement of aerosol particles affected by heat fluxes — the upward one from the surface and the downward one — at the inversion base

$$\omega_t(z) = \begin{cases} \alpha_t \langle \omega' \Theta' \rangle (z - h_0), & z < h_0, \\ 0, & z \geq h_0. \end{cases} \quad (22)$$

Here  $h_0 = 5h_1/6$  is the height of zero heat flux  $\langle \omega' \Theta' \rangle$  in the ML (see Fig. 1c);  $\alpha_t$  is the proportionality coefficient between  $\omega_t$  and  $\langle \omega' \Theta' \rangle$ .

Thus, the vertical component of the organized movement velocity for the ML aerosol was numerically estimated as the sum of three principal components

$$\omega_1(z, R_1) = \omega_s(R_1) + \omega_d(z) + \omega_t(z) \quad (23)$$

To model the absolute humidity profile by our technique we considered only the one velocity component  $\omega_t(z)$ .

Note that since the values of the eddy heat flux  $\langle \omega' \Theta' \rangle$ , of the potential temperature  $\Theta(t)$ , and also of the layer depth  $h(t)$  are time dependent, the profiles of  $D(z)$  and  $\omega_1(z)$  must also depend on time

(see relationships (13)–(23)). Therefore the integral characteristics of the dispersed structure of the atmospheric haze  $N_1$ ,  $S_1$ , and  $V_1$  estimated from Eq. (12) are the functions of two variables: the elevation above the ground  $z$ , and the time  $t$ .

### RESULTS OF NUMERICAL SIMULATION

The process of entrainment of warmer air from above the inversion into the structure of (relatively cool, see Fig. 1c) ML is a typical feature of inversion evolution. It is reflected in the comparatively complex dynamics of relative humidity  $Q(t)$  at different heights (Fig. 3). The values of  $Q(z, t)$  were calculated from the profiles of absolute humidity and temperature using the Magnus relationship.<sup>9</sup>

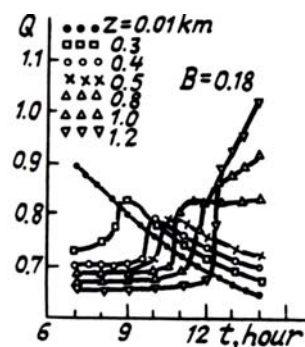


FIG. 3. Temporal dynamics of variations in relative humidity  $Q(z, t)$  at various heights within the ML.

A monotonic decrease of  $Q(t)$ , quite natural for the heated layer, is typical for those heights which constantly remain below the temperature inversion. The behavior dynamics of  $Q(z, t)$  at other heights is characterized by an abrupt change in the relative humidity value at the moment of entrainment of a given stratification into the ML.

Considering the large number of model parameters, a comprehensive study of the mechanism of surface haze variability remains outside the scope of any single report. Therefore our first step in applying these results was to consider the effect of gravitational sedimentation on spatial deformations of the size spectrum of the dispersed particles and, as a result, profiles of the parameters of the aerosol light scattering.

TABLE I.

| $R_t^*$ | $\omega_s^{**}$ | $R_1$ | $\omega_s$ | $R_1$ | $\omega_s$ |
|---------|-----------------|-------|------------|-------|------------|
| 0.027   | 2.0E-6          | 0.340 | 8.2E-5     | 1.887 | 2.1E-3     |
| 0.067   | 6.2E-6          | 0.742 | 3.5E-4     | 3.425 | 6.8E-3     |
| 0.106   | 1.2E-5          | 1.970 | 7.3E-4     | 4.615 | 1.2E-2     |

\*  $R_1$  is in  $\mu\text{m}$

\*\*  $\omega_s$  is in  $\text{m/s}$

Table I presents the values of  $\omega_s(R)$  calculated from Eq. (18), according to which the values of  $\omega_s$  for the coarse fraction (columns 5 and 6) exceed, by more than a factor of 100, similar values from the accumulative fraction (columns 3–4), and by more than 1000 – those from the photochemical fraction (columns 1–2).

Note that we considered not only the first-order gravitational sedimentation deformations of  $f(R, z, t)$ , related to fraction-by-fraction stratification of the integral profiles, but also the second-order effects produced by stratification of the spectrum moments within each separate fraction. i.e.,  $N_i(z, t)$ ,  $S_i(z, t)$ ,  $V_i(z, t)$ .

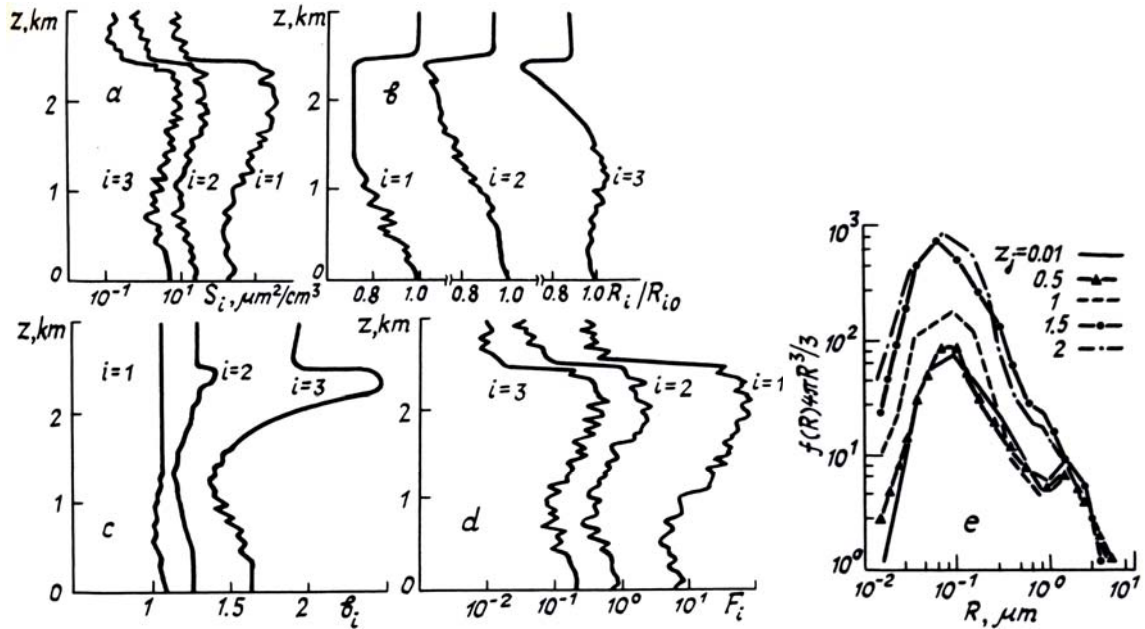


FIG. 4. Model vertical profiles of the aerosol microphysical parameters in the mixing layer. a) vertical profiles of the particle integral cross sections for three fractions,  $S_i(z)$ ,  $i = 1, 2, 3$ . b) vertical profiles of model radii for three fractions  $R_i(z)/R_i(z = 0)$ . c) vertical profiles of the parameters  $b_i(z)$  (model (7)). d) vertical profile of the parameters  $F_i(z)$  (model (7)). e) examples of model spectra  $f(R, z, t)$  at various heights:  $z_j = 0.0, 0.5, 1.0, 1.5, 2.0$  km calculated for  $t = 14:00$  LT.

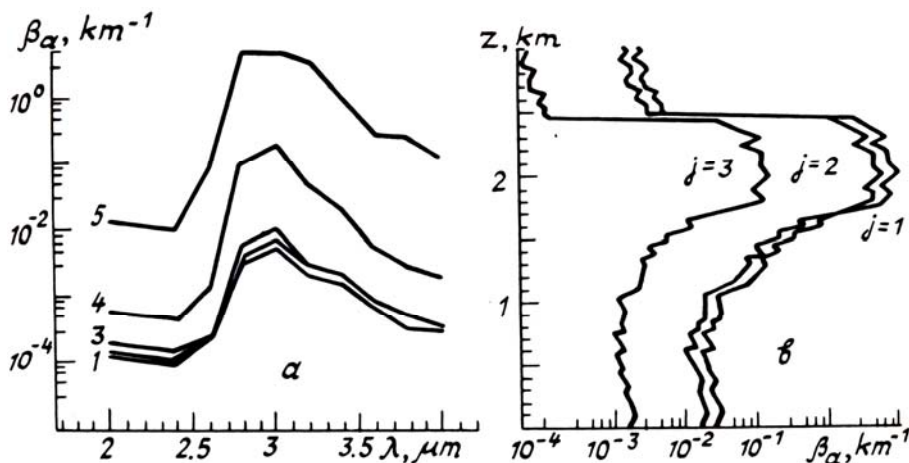


FIG. 5. Altitude transformations of light scattering parameters for atmospheric aerosol in the mixing layer: a) vertical profile of the absorption coefficient  $\beta_a(z, \lambda_j)$  for  $\lambda_j = 3.2, 3.4, 3.6 \mu\text{m}$ ; b) vertical transformation of the spectral dependence of absorption coefficient within the layer for  $z_j = 0.0, 0.5, 1.0, 1.5, 2.0$  km.

This approach makes it possible to separate theoretically dynamic variations in such traditional parameters of the spectra as  $R_1(z, t)$  and  $b_1(z, t)$ , which characterize the size and width of the distributive mode of the particles for each  $i$ -th fraction.

Within the ML the integral characteristics of the fine fraction of haze display a stable growth tendency with height when vertical heat fluxes from the surface are of an organized nature (Fig. 4a), while the coarse particle concentration can at least be homogeneously distributed with height.

Noticeable deformations are suffered by the size spectrum itself. In particular, the modal radii of all three fractions consistently decrease with height. For coarse particles this decrease reaches as much as 20%. Also the width of the distributive mode changes from  $b_1 = 1.6$  to 2.1 (Fig. 4b, c). Vertical profiles of the  $F_1(z)$  parameters describe the dynamics of quantitative variations for each fraction in sharper relief than the parameters  $N_1(z)$ ,  $S_1(z)$ , and  $V_1(z)$  themselves (Fig. 4d).

The above regularities are valid even upon introducing random 50% deviations into the computed average profiles of the integral characteristics  $N_1(z)$ ,  $S_1(z)$ ,  $F_1(z)$ .

Figure 4e shows several examples of the aerosol size spectrum, illustrating variations of the dispersed haze structure with height.

Computations of the model optical characteristics following from the varying microstructure of haze were performed taking into account the local relative humidity. This consideration emphasized the typical stratification features of light scattering below the inversion (Fig. 5a).

The analysis of the spectral dependence of optical characteristics performed, using two model options for the complex index of refraction of the atmospheric aerosol,<sup>7</sup> demonstrates (see Fig. 5) that the strongest variations in light scattering occur around the typical absorption bands of an aerosol, particularly, water.

Thus in the sub-inversion zone the aerosol absorption coefficient at  $\lambda = 2.8 \mu\text{m}$  can increase by more than three orders of magnitude from its ordinary surface value; indeed, the relative humidity here can, in certain cases, reach the dew point, so that aerosol particles would grow up to sizes typical for water-droplet fogs. In that case (see Fig. 5b) spectral irregularity of the absorption coefficient extends to adjacent wavelengths too. While at the surface the value of  $\beta_a$  ( $\lambda = 2.8 \mu\text{m}$ ) exceeds that of  $\beta_a$  ( $\lambda = 2.0 \mu\text{m}$ ) by a factor of ten, the respective excess in the sub-inversion zone is larger than a factor of 100.

A complex temporal variability of optical characteristics is also observed. Daytime heating lowers relative humidity in the surface atmospheric layers, resulting in a monotonic decrease of their aerosol absorption coefficient. Accumulation of the aerosol in the sub-inversion zone, combined with the above-mentioned abrupt change in relative humidity (when

the layers above the inversion are entrained into the ML structure) lead to strong irregularity in the aerosol light scattering at these heights.

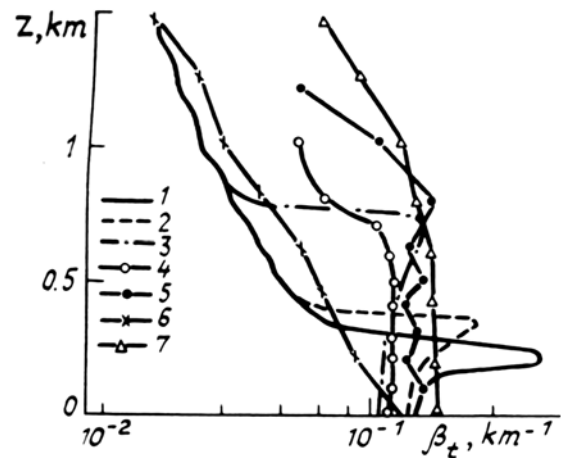


FIG. 6. Temporal deformations of the vertical profile of the aerosol extinction coefficient ( $\lambda = 0.53 \mu\text{m}$ ): 1–3 – model computations for  $t_j = 8:00, 9:30, 12:30$  LT; 4, 5 – experimental data;<sup>12</sup> 6, 7 – model estimates obtained earlier.<sup>4</sup>

The temporal transformation of the vertical profile of the volume aerosol extinction coefficient, calculated for  $\lambda = 0.53 \mu\text{m}$  at  $B = 0.18 \text{ deg} \cdot \text{m/s}$ , is presented in Fig. 6 vs. experimental data (curves 4 and 5<sup>12</sup>) and earlier numerical simulation results (curves 6, 7<sup>4</sup>). The calculated data illustrate quite well the anomalous accumulation of aerosol matter in the sub-inversion zone during morning hours and the subsequent gradual decrease of turbidity in the surface layer.

Simulations demonstrate that the rate and character of deformations suffered by the surface layer haze in its structure depend significantly on the initial parameter of the process, i.e., the initial temperature profile  $\Theta_0(z)$ , heat flux from the surface  $\langle \omega' \Theta' \rangle_0$ , frictional velocity  $u_*$ , etc. Therefore, the estimates presented above only illustrate overall tendencies in the state of the aerosol component in the ML; they should not be regarded as all-embracing and final descriptions.

## CONCLUSION

A model forecasting technique for the dynamics of optical properties of the dispersed component of the atmospheric surface layer, developed in the present paper, consists of three principal elements. The reductional description of the particle size spectrum of the atmospheric haze (7)–(11) using its integral characteristics, can be considered as a fundamentally new approach. In a sense it combines and relates the model of ML (1)–(6), which describes the state and development of the carrier medium, and Eqs. (12)–(23), which control the aerosol flux budget within

the layer and, hence, the redistribution processes of different fractions with height.

Obviously, certain conceptual simplifications had to be implicitly agreed upon at every step of describing these processes of varying scales, necessitated by the severe difficulties one would face in attempting to formulate each intermediate step rigorously and to solve the general problem trying to obtain practical results.

This paper considers the effect of gravitational sedimentation only. However, it is clear that the suggested modeling technique can be tested in comparative theoretical vs. experimental studies of the role of other geophysical factors in these processes. In particular, the model estimates with the specific formation conditions of the eddy heat flux  $\langle \omega' \theta' \rangle$ , its intensity and diurnal variations taken into account can be of practical interest. Such simulations and comparisons would undoubtedly depend on the season and climatic zone, and they would be instrumental in estimating the regional features of the atmospheric haze.

#### REFERENCES

1. H.J. Tennekes, *Atmos. Sci.* **30**, 558 (1973).
2. F.K. Boll, *Quart. J. Roy. Meteor. Soc.* **86**, 483 (1960).
3. D.K. Lilly, *Quart. J. Meteor. Soc.* **94**, 292 (1968).
4. G.M. Krekov and R.F. Rakhimov, *Optical Models of the Atmospheric Aerosol* (Tomsk Affiliate of the Siberian Branch of the Academy of Sciences of the USSR, Tomsk, 1986).
5. R.F. Rakhimov, *Atm. Opt.* **2**, No. 3, 259 (1989).
6. G. Hanel, *Adv. in Geophys.* **19**, 73 (1976).
7. L.S. Ivlev, and S.D. Andreev, *Optical Properties of the Atmospheric Aerosol* (LSU, Leningrad, 1986).
8. V.F. Derr, *Remote Sensing of Troposphere*, (WPL ERL EED, Boulder, Colorado, 1972).
9. L.T. Matveev, *A Course of General Meteorology. Physics of the Atmosphere* (Gidrometeoizdat, Leningrad, 1976).
10. G.M. Krekov, and R.F. Rakhimov, *Optical-Radar Model of Continental Aerosol* (Nauka, Novosibirsk, 1982).
11. A. Goroch, S. Burk, and K.L. Davidson, *Tellus* **32**, 245 (1980).
12. V.V. Balakirev, Yu.O. Dyabin, et al., in: *Abstracts of Reports at the Fifth All-Union Symp. on Laser and Acoustic Sounding of the Atm.* (Institute of Atmospheric Optics, Siberian Branch of the Academy of Sciences of the USSR, Tomsk, 1978).